



Published in final edited form as:

*Bioorg Med Chem Lett.* 2015 November 1; 25(21): 4843–4847. doi:10.1016/j.bmcl.2015.06.048.

## A multifunctional, light-activated prochelator inhibits UVA-induced oxidative stress

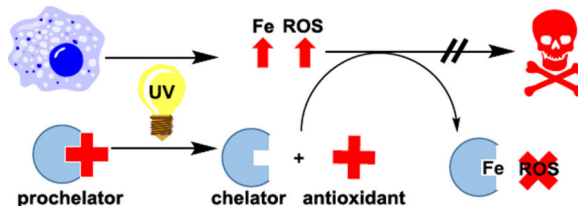
Andrew T. Franks, Qin Wang, and Katherine J. Franz\*

Duke University, Department of Chemistry, 124 Science Dr., Durham, NC 27708, USA.

### Abstract

UVA radiation can damage cells and tissues by direct photodamage of biomolecules as well as by initiating metal-catalyzed oxidative stress. In order to alleviate both concerns simultaneously, we synthesized a multifunctional prochelator PC-HAPI (2-((E)-1-(2-isonicotinoylhydrazono)ethyl)phenyl (trans)-3-(2,4-dihydroxyphenyl)acrylate) that contains a trans-(o-hydroxy)cinnamate ester photocleavable protecting group that is cleaved upon UVA exposure to release a coumarin, umbelliferone, and an aroylhydrazone metal chelator, HAPI (N'-[1-(2-hydroxyphenyl)ethylidene]isonicotinoylhydrazide). While the prochelator PC-HAPI exhibits negligible affinity for iron, it responds rapidly to UVA irradiation and converts to an iron-binding chelator that inhibits iron-catalyzed formation of reactive oxygen species and protects cells from UVA damage.

### Graphical abstract



### Keywords

chelator; photocleavage; oxidative stress; UVA damage; antioxidant

Radiation in the ultraviolet A (UVA) range (320–400 nm) of the electromagnetic spectrum is a contributor to skin and retinal tissue damage associated with aging.<sup>1–3</sup> These longer UV wavelengths pass through the atmosphere and penetrate more deeply into biological tissues than the shorter UVB wavelengths (290–320 nm). A number of biological chromophores

\*Tel: +1(919) 660 1541; katherine.franz@duke.edu.

**Publisher's Disclaimer:** This is a PDF file of an unedited manuscript that has been accepted for publication. As a service to our customers we are providing this early version of the manuscript. The manuscript will undergo copyediting, typesetting, and review of the resulting proof before it is published in its final citable form. Please note that during the production process errors may be discovered which could affect the content, and all legal disclaimers that apply to the journal pertain.

Supplementary Material

Supplementary material is available for download and includes all experimental details and supporting data figures mentioned in the main text.

absorb UVA light, including enzyme cofactors (e.g. porphyrins and flavins), pigments (eumelanin and pheomelanin) and other amino acid derived species.<sup>4-6</sup> In addition to dissipating the absorbed energy through photon emission or radiationless decay, these excited chromophores can propagate reactive excited states in neighboring biomolecules via energy transfer mechanisms and further stress cellular systems via reaction with molecular oxygen to form singlet oxygen, superoxide and hydrogen peroxide.<sup>7-9</sup>

UVA radiation is also known to cause cell damage via iron-dependent mechanisms.<sup>10,11</sup> Exposure of fibroblasts and keratinocytes to environmentally relevant doses of UVA has been shown to release iron (Fe) from cellular stores in both ferritin and heme.<sup>12</sup> While normal fluctuations in cellular Fe are moderated by homeostatic machinery, the amount of reactive Fe that is released from moderate to severe UVA exposure can overwhelm this natural Fe buffering system. Iron that is not regulated sufficiently can undergo Fenton chemistry and generate highly reactive hydroxyl radicals as well as alkoxy and peroxy radicals.<sup>13-15</sup> These reactive oxygen species (ROS) can damage DNA, proteins and lipids with diffusion-limited kinetics. Several studies have shown, however, that oxidative damage induced by both light and Fe can be alleviated by treatment with chelating agents.<sup>10,16-21</sup>

While the clinical benefits of chelation therapy are clear for remediation of some select diseases associated with Fe overload, care must be taken to avoid the unintended consequences of altering systemic metal balances.<sup>22</sup> Basal levels of Fe are required for cellular respiration and other crucial cellular processes; therefore, systemic loss of Fe and long-term disruption of homeostasis by chelating agents could also cause harm.<sup>23-25</sup> A prochelator strategy with responsive unmasking and selective targeting of only unregulated and damaging species of Fe is desirable to avoid possible side effects from systemic metal depletion.<sup>26,27</sup> Pourzand et al. introduced a light-activated protecting moiety to mask the key metal-binding oxygen of two extensively studied chelators, salicylaldehyde isonicotinoyl hydrazone (SIH) and pyridoxal isonicotinoyl hydrazone (PIH) to afford corresponding prochelators with negligible Fe affinity.<sup>28</sup> Irradiation of the prochelators with UVA wavelengths effects an intramolecular oxygen transfer within the (*o*-nitrobenzyl)ethyl protecting group with a concomitant release of active SIH or PIH. In this way, only labile Fe that is present near sites of UVA exposure is targeted for chelation. However, while this strategy has been suitable for biochemical studies in the lab, concerns persist about possible cytotoxic effects from the nitrosoketone by product released as a result of uncaging.<sup>29</sup>

In our search for an alternative uncaging strategy with concomitant release of functional yet nontoxic components, we reasoned that a *trans*-(*o*-hydroxy)cinnamate ester photocleavable protecting group that releases a coumarin photoproduct would be favorable.<sup>30-34</sup> Coumarins are among several classes of abundant and potent plant-based antioxidants.<sup>35,36</sup> The diversity of substituents around the heterocyclic core of natural coumarins have inspired structure-activity studies to explore and compare their antioxidant potency.<sup>37-41</sup> Among the simplest structures of plant coumarins is 7-hydroxycoumarin, also known as umbelliferone, which is believed to be one of the active ingredients in several medicinal plant extracts.<sup>42-44</sup> Moreover, the purported antioxidant activity of coumarins complements that of antioxidant chelating agents. As sacrificial antioxidants, coumarins mitigate oxidative stress by quenching oxygen-based radicals stoichiometrically, while effective chelators prevent

redox-active metal ions from catalytically generating such radicals in the first place. Since both direct UV damage of biomolecules and catalytic production of hydroxyl radicals by Fe contribute to UVA photodamage, a single molecule that could mitigate both concerns may prove more effective than treating either cause individually.

In the present report, a multifunctional prochelator has been developed to address the simultaneous concerns of both Fe-catalyzed and direct generation of ROS due to UVA exposure. The compound PC-HAPI is designed using a “photocaged” prochelator strategy. In this design, irradiation cleaves a photolabile protecting group to yield the active form of a chelator, in this case the lipophilic aroylhydrazone HAPI. An *o*-hydroxycinnamic acid photoprotecting group has been chosen to release the coumarin umbelliferone upon activation (Scheme 1). Umbelliferone not only exhibits strong UVA absorption, but is also reported to possess antioxidant properties.<sup>37,38,40,41,44</sup>

PC-HAPI was synthesized by following a synthetic scheme modified from published *o*-hydroxycinnamate protections.<sup>30,45,46</sup> Wittig chemistry was used to generate a *trans*-cinnamate ester. Allyl ether protection of the cinnamate protecting group was used to enable coupling with the HAPI phenolate while avoiding unproductive reactions of the cinnamate with itself. Coupling of the cinnamate protecting group to HAPI was done by in situ generation of a cinnamoyl chloride and aryl ester formation in pyridine solution (Figure S1). The product was obtained as a pale yellow solid that dissolves readily in halogenated solvents and is suitably soluble in DMSO for preparation of stock solutions in the millimolar concentration range.

Photoinduced changes in the absorption spectrum of PC-HAPI were monitored by UV-visible absorption spectrophotometry (Figure 1). For comparison, authentic samples of HAPI and ethyl (*E*)-3-(2,4-dihydroxyphenyl)acrylate (compound **1**)<sup>47</sup> were also monitored to assess the independent response of the aroylhydrazone framework and the cinnamate protecting group, respectively, to UVA exposure. Samples in pH 7.4 buffered aqueous solution were irradiated under a 4 W handheld UV lamp for 15 s intervals, which triggered a decrease in absorbance of PC-HAPI at 284 and 350 nm with a concomitant increase of a new feature at 325 nm. Three clean isosbestic points are apparent, suggesting the photoconversion proceeds in one step without side products or long-lived intermediates. The solution was irradiated until no further changes were observed (60 s), resulting in a final absorption spectrum that matches the spectrum of a solution containing equimolar quantities of authentic samples of umbelliferone and HAPI. Irradiation of HAPI itself under these conditions also results in spectral changes, as depicted by the subtle decreases in absorption in Figure 1c. These changes can be attributed to partial *E-Z* isomerization of the HAPI hydrazone bond, which we previously reported.<sup>48</sup> The intensity and duration of irradiation in the current experiment is clearly not sufficient to fully photoisomerize the HAPI sample, as the metastable *Z* isomer has very little absorption at 400 nm.<sup>48</sup> Interestingly, the spectrum of PC-HAPI does not continue to lose absorbance at 400 nm upon longer irradiation times, suggesting that the coumarin chromophore may inhibit HAPI photoisomerization by a filter effect.

Coumarins are recognized for their fluorescence properties, so we anticipated observing an increase in fluorescence upon release of umbelliferone during photodeprotection of PC-HAPI. Emission spectra were collected for PC-HAPI before and after incremental exposure to UVA radiation. As shown in Figure 2, a pre-UVA solution is only weakly fluorescent, but after 10 s of UVA exposure a strong growth in emission is observed from the irradiated PC-HAPI solution. No further increases were observed after 60 s of UVA exposure. The final spectrum collected exhibits a 4-fold increase in emission over the initial spectrum and matches an umbelliferone standard of the same concentration.

In order to fully characterize the products of photoreaction, the starting materials and products were analyzed by NMR spectrometry (Figure S2) and liquid chromatography-mass spectrometry (LC-MS) (Figure 3). Both methods show the clean conversion of PC-HAPI to HAPI and umbelliferone. LC-MS analysis of PC-HAPI solutions before and after UVA irradiation shows the UV-induced decrease in [PC-HAPI] with concomitant appearance of two new major peaks at 8.3 min and 11.6 min. The elution times and corresponding mass spectra for these peaks match authentic samples of umbelliferone and HAPI, respectively. A minor species appearing earlier in the run has a corresponding parent ion mass-to-charge ratio of 256, which is also consistent with the molecular mass of HAPI. We assign this peak as the (Z)-HAPI photoisomer.<sup>48</sup> These results support the proposed uncaging mechanism depicted in Scheme 1, wherein absorption of UVA wavelengths of light induces *cis-trans* isomerization of the cinnamate olefin. Isomerization allows for intramolecular nucleophilic substitution that releases HAPI and generates a fluorescent coumarin species.

The quantum yield of photolysis ( $\Phi_p$ ) for the PC-HAPI photoreaction was determined by using LC-MS. The extent of PC-HAPI photolysis was compared under identical conditions to that of compound **1**, for which  $\Phi_p$  is known. The quantum yield was found to be  $8.1 \pm 0.2\%$ , which is slightly less than the value determined for compound **1** (9%), which has the same protecting group moiety but with an ethanol leaving group.<sup>47</sup>

A functional prochelator should have a low metal affinity until acted on by the trigger stimulus, which releases a strong chelating species. To assess the metal binding behavior of PC-HAPI before and after UV irradiation, the fluorescent metal ligand calcein was used as a competitive chelator in a microplate assay. Coordination of  $\text{Fe}^{3+}$  quenches the fluorescence of calcein, so a competing chelator can restore calcein emission by binding the metal and releasing free calcein. As seen in Figure 4, quenched Fe(calcein) solutions treated with HAPI show a strong return of fluorescence as  $\text{Fe}^{3+}$  is efficiently removed from its complex with calcein. Treatment with the prochelator PC-HAPI fails to restore emission, indicating that the Fe affinity of HAPI has been attenuated by the photolabile masking group. Treatment of Fe(calcein) with a solution of PC-HAPI that was irradiated under UVA light prior to mixing results in near complete restoration of calcein fluorescence. The UVA-dependent increase in calcein fluorescence following treatment with PC-HAPI indicates the release of an active chelator that is able to compete with calcein for chelatable Fe.

Given that PC-HAPI exhibits favorable prochelator properties, we further tested its effectiveness for inhibiting Fe-dependent formation of ROS. In the absence of suitably deactivating ligands, hydrogen peroxide oxidizes  $\text{Fe}^{2+}$  to  $\text{Fe}^{3+}$  and generates hydroxyl

radical in aqueous solutions. If a reducing agent is also present to recycle  $\text{Fe}^{3+}$  back to  $\text{Fe}^{2+}$ , this reaction can be catalytic in Fe, resulting in dramatically increased ROS production that can be measured by the two-electron oxidation of non-fluorescent dihydrodichlorofluorescein ( $\text{H}_2\text{DCF}$ ). The fluorescence emission of the oxidation product dichlorofluorescein (DCF) can thus be monitored to assess a compound's affect on ROS production. If a protective affect is observed at low compound concentrations, it can indicate the presence of an Fe chelator that prevents catalytic ROS formation, whereas compounds that diminish DCF fluorescence at higher concentrations can indicate a capability of quenching the ROS that forms. Solutions containing  $\text{H}_2\text{DCF}$  were incubated with  $\text{Fe}^{3+}$ , hydrogen peroxide, ascorbic acid and nitrilotriacetic acid (NTA, used to keep Fe in solution). As shown by the bar on the far right in Figure 5, these conditions generate significant DCF fluorescence. Treated wells were dosed with HAPI or PC-HAPI with (+) or without (-) UVA irradiation. Emission levels from wells containing only  $\text{H}_2\text{DCF}$  and buffer were stable over the time period of the experiment, and this background emission was subtracted from readings for all control and treatment wells.

DCF emission of solutions treated with HAPI decreased in a dose-dependent manner (Figure 5). This behavior is consistent with the protective effects observed in previous studies of HAPI and related aroylhydrazone chelators, where sequestration of the active metal center inhibits ROS production.<sup>49-52</sup> Wells treated with non-irradiated PC-HAPI show much higher levels of DCF emission, with a decrease observed only at the highest 200  $\mu\text{M}$  dose. This result indicates that PC-HAPI itself does not prevent Fe-catalyzed ROS production, but may provide antioxidant properties of ROS quenching at high concentrations. Emission drops markedly in wells treated with irradiated PC-HAPI compared to wells containing the same concentration of non-irradiated PC-HAPI. The light-dependent DCF emission levels suggest that PC-HAPI is unable to prevent Fe redox cycling until it is activated by UVA radiation. The photolyzed sample, on the other hand, shows inhibition of Fe redox catalysis at low to moderate concentrations. However, the 100  $\mu\text{M}$  and 200  $\mu\text{M}$  photolyzed PC-HAPI samples still exhibit some DCF fluorescence and therefore do not fully replicate the behavior observed with corresponding HAPI solutions, which show negligible DCF emission.

In order to further probe why irradiated samples of PC-HAPI do not fully prevent DCF fluorescence, the other PC-HAPI photoproduct, umbelliferone, was also examined by this assay (Figure 6).  $\text{H}_2\text{DCF}$  solutions containing the same ROS-generating reagents were treated with a range of umbelliferone concentrations and, for comparison, the water-soluble antioxidant trolox (6-hydroxy-2,5,7,8-tetramethylchroman-2-carboxylic acid). Whereas trolox effectively inhibits DCF oxidation under these conditions, umbelliferone shows a dose-dependent *increase* in DCF emission. Because of the very different excitation and emission profiles of umbelliferone and DCF, this growth in emission is not due to umbelliferone fluorescence itself. This result suggests that umbelliferone promotes, rather than quenches, ROS production under these Fenton-like conditions. While this behavior is unexpected and is incongruous with the reported antioxidant behavior of coumarin phenols, it is only observed at much higher concentrations than would be administered in a biological application.

To investigate the potency of PC-HAPI to protect cells subjected to UVA damage, retinal pigment epithelial ARPE-19 cells were chosen as they suffer from UVA-induced oxidative stress during age-related macular degeneration (AMD).<sup>53</sup> As indicated in Figure 7, cells exposed to UVA irradiation were protected from cell death by both HAPI and PC-HAPI, while umbelliferone itself provided little protection. HAPI was protective at all concentrations tested from 5 to 100  $\mu\text{M}$ , while PC-HAPI showed greatest protection against UV damage at doses lower than 50  $\mu\text{M}$ , with less protection at the higher doses. Cytotoxicity studies revealed that PC-HAPI, HAPI, and umbelliferone were nontoxic at concentrations up to 100  $\mu\text{M}$  after 24 h incubation. ARPE-19 cells were less tolerant of high doses of HAPI and PC-HAPI when incubation was extended over 72 h, although doses below 25  $\mu\text{M}$  showed minimal toxicity even after 72 h.

In summary, we seek to improve upon previous efforts to sequester reactive Fe using light-triggered prochelators by releasing not only one but two functional photoproducts with useful properties for attenuating UV photodamage. The newly synthesized compound PC-HAPI responds sensitively to UVA exposure, releasing both the coumarin umbelliferone and the aroylhydrazone metal chelator HAPI. The prochelator PC-HAPI has weakened affinity for Fe due to the acylation of the metal-binding phenolate oxygen. Upon exposure to UVA radiation, the free phenol is released and restores the affinity for Fe. Assays of Fe-catalyzed ROS generation using dihydrodichlorofluorescein indicate that the released chelator HAPI attenuates ROS generation, while umbelliferone may act as a pro-oxidant at high concentrations. Cell studies further demonstrate that PC-HAPI and its corresponding chelator HAPI effectively protect retinal pigment epithelial cells from UVA irradiation. In contrast, the insignificant cytoprotective effect of umbelliferone is likely to derive from its pro-oxidant potential. The activity of several other naturally occurring and synthetic coumarins have identified numerous compounds with highly potent antioxidant and anti-inflammatory activity. Future iterations of cinnamate-protected prochelators could be designed to release these potent coumarins and thus confer greater protective effects against harmful UV damage.

## Supplementary Material

Refer to Web version on PubMed Central for supplementary material.

## Acknowledgement

We thank the National Institutes of Health (RO1-GM084176) and the National Science Foundation (CHE-1152054) for supporting various aspects of this work.

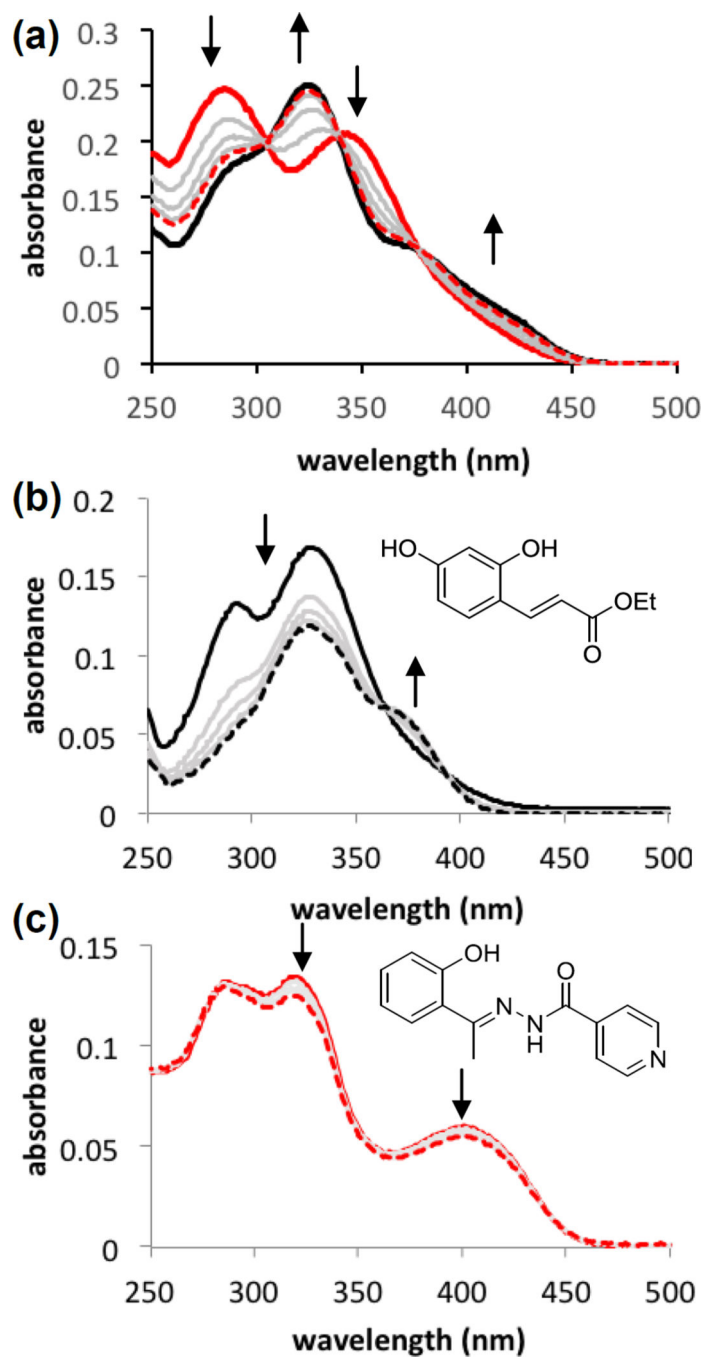
## References

1. Rapp L, Tolman B, Dhindsa H. Invest. Ophthalmol. Vis. Sci. 1990; 31:1186. [PubMed: 2354921]
2. Stark WS, Tan KEWP. Photochem. Photobiol. 1982; 36:371. [PubMed: 6755502]
3. Boulton M, Ró anowska M, Ró anowski B. Photochem. Photobiol. B. 2001; 64:144.
4. Cunningham ML, Johnson JS, Giovanazzi SM, Peak MJ. Photochem. Photobiol. 1985; 42:125. [PubMed: 2996041]
5. Peak J, Peak M, MacCoss M. Photochem. Photobiol. 1984; 39:713. [PubMed: 6429679]
6. Young AR. Phys. Med. Biol. 1997; 42:789. [PubMed: 9172259]

7. Trautinger F. *Clin. Exp. Dermatol.* 2001; 26:573. [PubMed: 11696060]
8. Miyachi Y. *J. Dermatol. Sci.* 1995; 9:79. [PubMed: 7772578]
9. Scharffetter-Kochanek K, Wlaschek M, Brenneisen P, Schauen M, Blandschun R, Wenk J. *Biol. Chem.* 1997; 378:1247. [PubMed: 9426184]
10. Bissett DL, Chatterjee R, Hannon DP. *Photochem. Photobiol.* 1991; 54:215. [PubMed: 1780358]
11. Jurkiewicz BA, Buettner GR. *Photochem. Photobiol.* 1994; 59:1. [PubMed: 8127935]
12. Pourzand C, Watkin RD, Brown JE, Tyrrell RM. *Proc. Natl Acad. Sci. USA.* 1999; 96:6751. [PubMed: 10359784]
13. Halliwell B, Gutteridge J. *Biochem. J.* 1984; 219:1. [PubMed: 6326753]
14. Halliwell B, Gutteridge JMC. *FEBS Lett.* 1992; 307:108. [PubMed: 1322323]
15. Walling C. *Acc. Chem. Res.* 1975; 8:125.
16. Mitani H, Koshiishi I, Sumita T, Imanari T. *Eur. J. Pharmacol.* 2001; 411:169. [PubMed: 11137872]
17. Richardson DR, Ponka P. *J. Lab. Clin. Med.* 1998; 132:351. [PubMed: 9794707]
18. Horackova M, Ponka P, Byczko Z. *Cardiovasc. Res.* 2000; 47:529. [PubMed: 10963725]
19. Santos NCF, Castilho RF, Meinicke AR, Hermes-Lima M. *Eur. J. Pharmacol.* 2001; 428:37. [PubMed: 11779035]
20. Chaston TB, Richardson DR. *Am. J. Hematol.* 2003; 73:200. [PubMed: 12827659]
21. Seite S, Popovic E, Verdier MP, Roguet R, Portes P, Cohen C, Fourtanier A, Galey JB. *Photoderm. Photoimmunol. Photomed.* 2004; 20:47.
22. Charkoudian LK, Dentchev T, Lukinova N, Wolkow N, Dunaief JL, Franz KJ. *J. Inorg. Biochem.* 2008; 102:2130. [PubMed: 18835041]
23. Dunaief JL. *Invest. Ophthalmol. Vis. Sci.* 2006; 47:4660. [PubMed: 17065470]
24. Duce JA, Bush AI. *Prog. Neurobiol.* 2010; 92:1. [PubMed: 20444428]
25. Rodríguez-Rodríguez C, Telpoukhovskaia M, Orvig C. *Coord. Chem. Rev.* 2012; 256:2308.
26. Reelfs O, Eggleston IM, Pourzand C. *Curr. Drug Metabol.* 2010; 11:242.
27. Perez LR, Franz KJ. *Dalton Trans.* 2010; 39:2177. [PubMed: 20162187]
28. Yiakouvaki A, Savovic J, Al-Qenaie A, Dowden J, Pourzand C. *J. Invest. Dermatol.* 2006; 126:2287. [PubMed: 16710308]
29. Kazanis S, McClelland RA. *J. Am. Chem. Soc.* 1992; 114:3052.
30. Turner AD, Pizzo SV, Rozakis GW, Porter NA. *J. Am. Chem. Soc.* 1987; 109:1274.
31. Turner AD, Pizzo SV, Rozakis G, Porter NA. *J. Am. Chem. Soc.* 1988; 110:244.
32. Porter NA, Bruhnke JD. *Photochem. Photobiol.* 1990; 51:37. [PubMed: 2304978]
33. Stoddard BL, Bruhnke J, Koenigs P, Porter N, Ringe D, Petsko GA. *Biochemistry.* 1990; 29:8042. [PubMed: 2261462]
34. Stoddard BL, Bruhnke J, Porter N, Ringe D, Petski GA. *Biochemistry.* 1990; 29:4871. [PubMed: 2364065]
35. Fylaktakidou KC, Hadjipavlou-Litina DJ, Litinas KE, Nicolaidis DN. *Curr. Pharm. Design.* 2004; 10:3813.
36. Bansal Y, Sethi P, Bansal G. *Med. Chem. Res.* 2013; 22:3049.
37. Gacche RN, Jadhav SG. *J. Exp. Clin. Med.* 2012; 4:165.
38. Hoult JRS, Payá M. *Gen. Pharmacol.* 1996; 27:713. [PubMed: 8853310]
39. Lin H-C, Tsai S-H, Chen C-S, Chang Y-C, Lee C-M, Lai Z-Y, Lin C-M. *Biochem. Pharmacol.* 2008; 75:1416. [PubMed: 18201686]
40. Paya M, Goodwin PA, De Las Heras B, Hoult JRS. *Biochem. Pharmacol.* 1994; 48:445. [PubMed: 8068031]
41. Paya M, Halliwell B, Hoult JRS. *Biochem. Pharmacol.* 1992; 44:205. [PubMed: 1322662]
42. Lino CS, Taveira ML, Viana GSB, Matos FJA. *Phytother. Res.* 1997; 11:211.
43. Vasconcelos JF, Teixeira MM, Barbosa-Filho JM, Agra MF, Nunes XP, Giulietti AM, Ribeiros-Santos R, Soares MBP. *Eur. J. Pharmacol.* 2009; 609:126. [PubMed: 19289114]
44. Singh R, Singh B, Singh S, Kumar N, Kumar S, Arora S. *Food Chem.* 2010; 120:825.

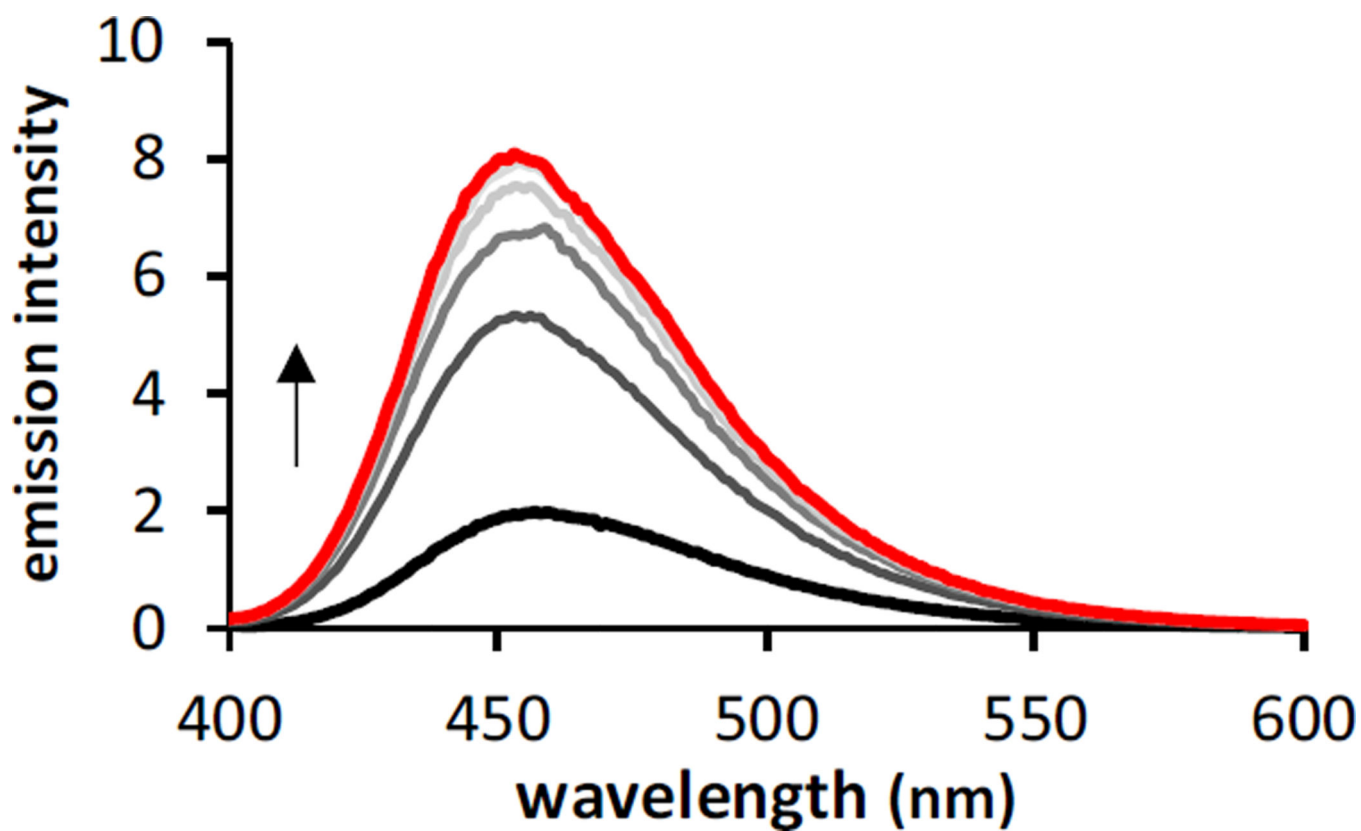
45. Porter NA, Thuring JW, Li H. *J. Am. Chem. Soc.* 1999; 121:7716.
46. Wijnmans M, Rosenthal SJ, Zwanenburg B, Porter NA. *J. Am. Chem. Soc.* 2006; 128:11720. [PubMed: 16939297]
47. Gagey N, Neveu P, Benbrahim C, Goetz B, Aujard I, Baudin J-B, Jullien L. *J. Am. Chem. Soc.* 2007; 129:9986. [PubMed: 17658803]
48. Franks AT, Peng D, Yang W, Franz KJ. *Inorg. Chem.* 2014; 53:1397. [PubMed: 24428136]
49. Kovacevic Z, Yu Y, Richardson DR. *Chem. Res. Toxicol.* 2011; 24:279. [PubMed: 21214214]
50. Bendova P, Mackova E, Haskova P, Vavrova A, Jirkovsky E, Sterba M, Popelova O, Kalinowski DS, Kovarikova P, Vavrova K, Richardson DR, Simunek T. *Chem. Res. Toxicol.* 2010; 23:1105. [PubMed: 20521781]
51. Hruskova K, Kovarikova P, Bendova P, Haskova P, Mackova E, Stariat J, Vavrova A, Vavrova K, Simunek T. *Chem. Res. Toxicol.* 2011; 24:290. [PubMed: 21214215]
52. Kielar F, Helsel ME, Wang Q, Franz KJ. *Metallomics.* 2012; 4:899. [PubMed: 22700084]
53. Chalam K, Khetpal V, Rusovici R, Balaiya S. *Eye & contact lens.* 2011; 37:225. [PubMed: 21646979]





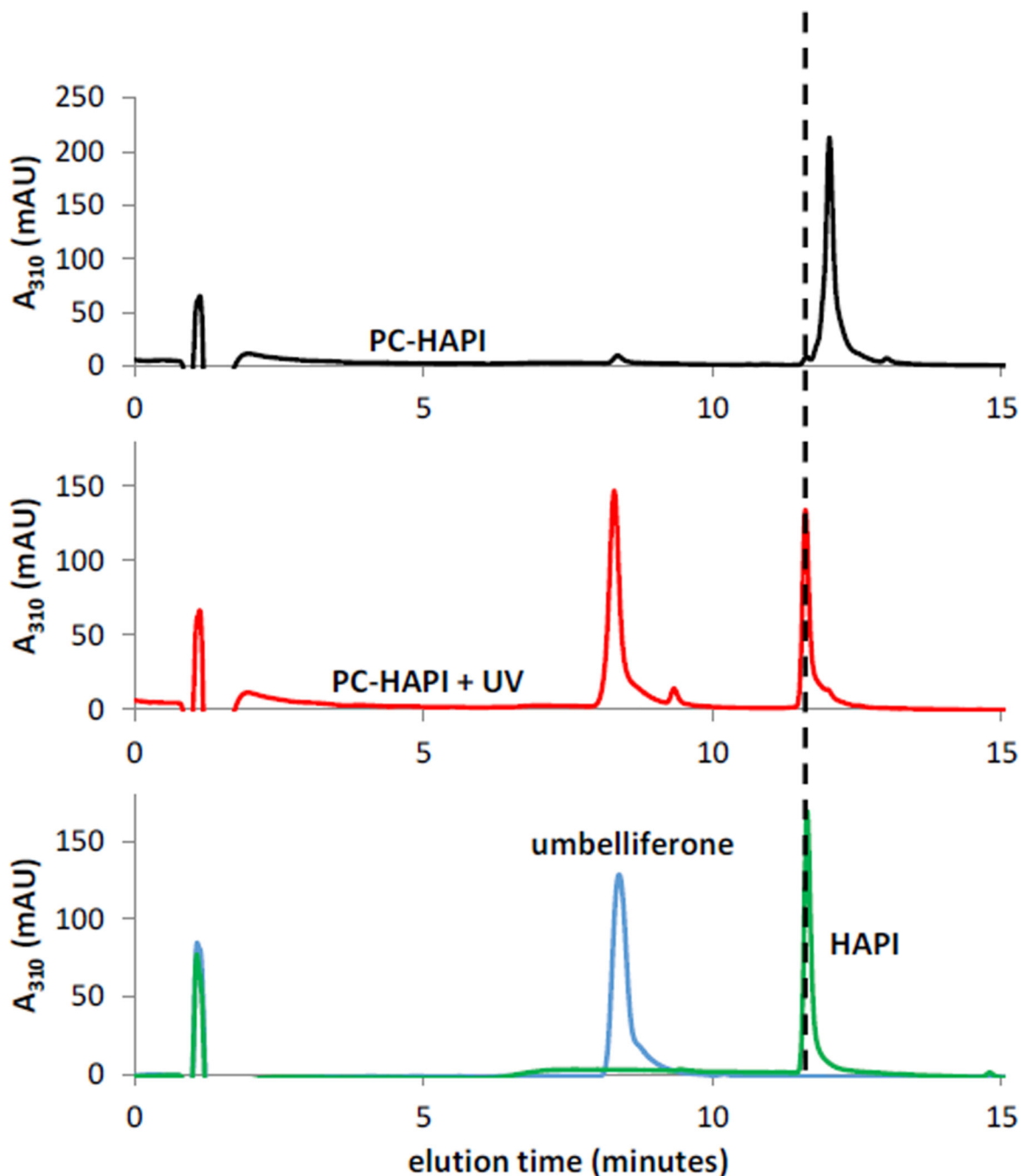
**Figure 1.**

Absorption spectra of (a) PC-HAPI, (b) compound **1**, and (c) HAPI in response to UVA irradiation. All solutions were prepared at 10 μM in pH 7.4 PBS buffer (<0.5% DMSO). Spectra prior to irradiation are shown as thick, solid lines; intermediate spectra taken after 15 s intervals of irradiation under a 4 W handheld lamp (maximum intensity at 366 nm) are shown as gray lines; final spectra recorded after 60 s total UV exposure are drawn as thick dashed lines. The final spectrum in the case of PC-HAPI (a) overlays with that of a solution containing a mixture of 10 μM umbelliferone and 10 μM HAPI (black, solid line).



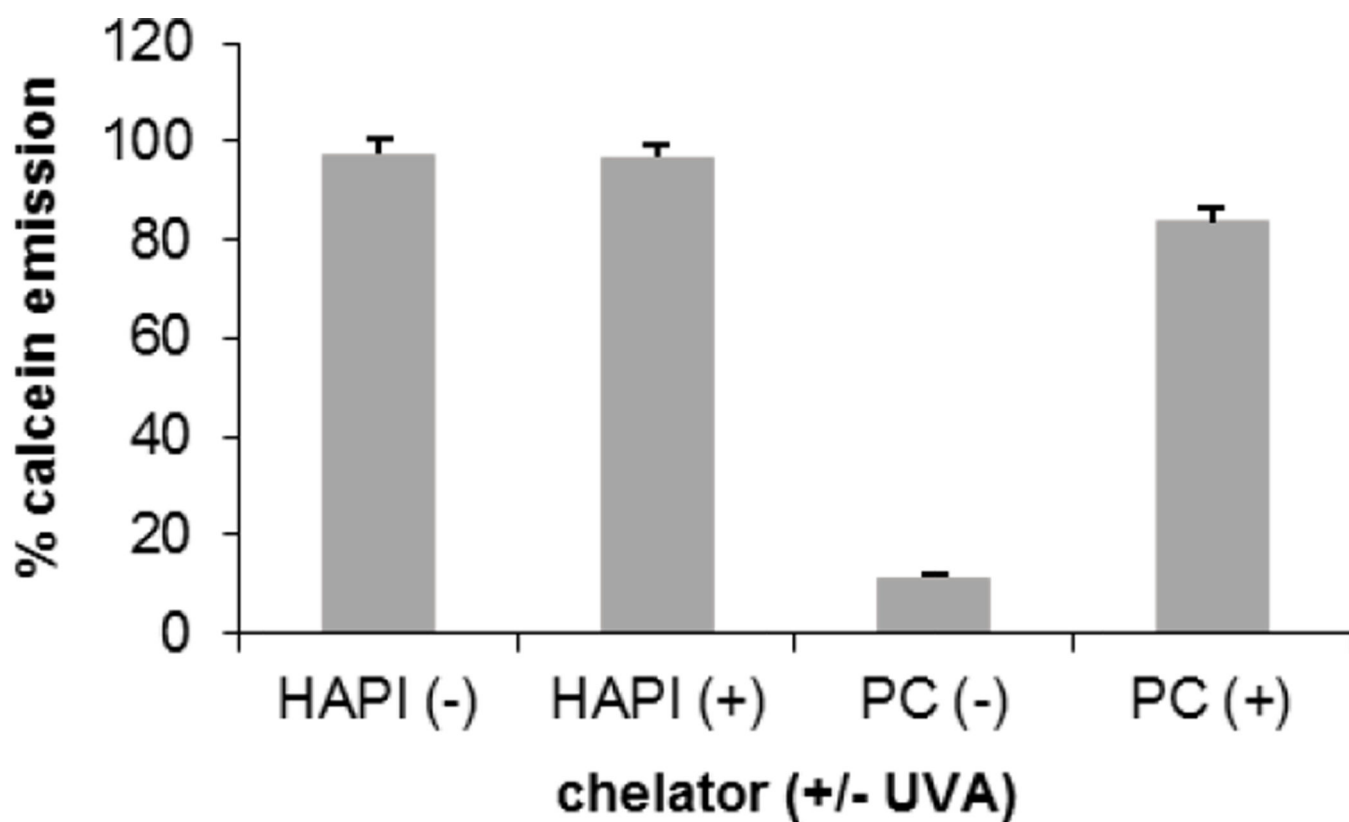
**Figure 2.**

Fluorescence emission of PC-HAPI increases upon exposure to UVA radiation. PC-HAPI is weakly fluorescent in aqueous solution prior to UVA exposure (black trace). Irradiation for 15, 30, 45, and 60 s (red trace) with UVA causes an increase in fluorescence. [PC-HAPI] = 1  $\mu$ M in PBS (0.1% DMSO)  $\lambda_{\text{ex}}$  = 360 nm. UVA irradiation was delivered by a 4W handheld lamp with maximum intensity at 366 nm.



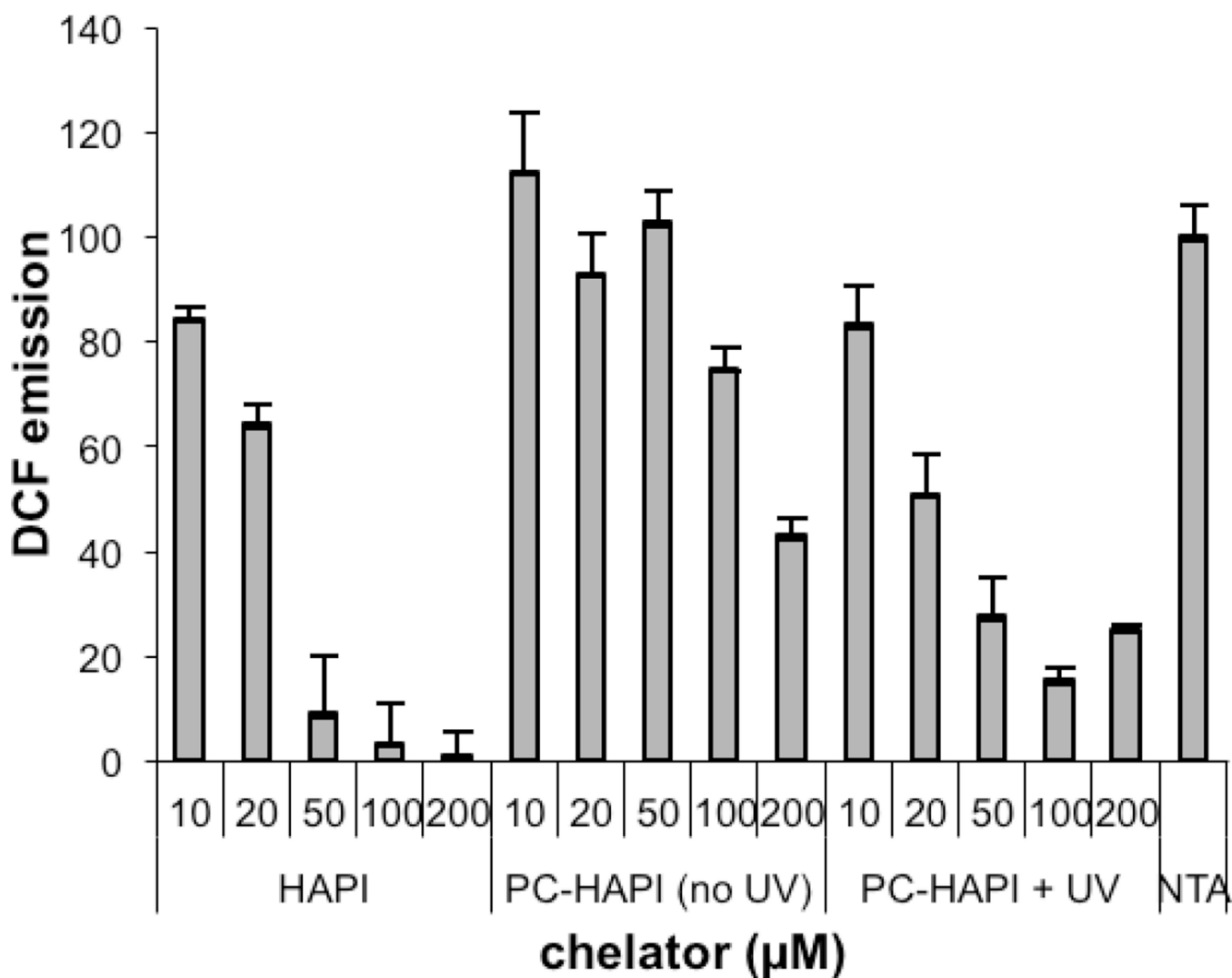
**Figure 3.**

UV-triggered conversion of PC-HAPI to umbelliferone and HAPI as monitored by LC-MS. **(top)** A solution of PC-HAPI kept in the dark elutes as a single peak at 12.0 min. **(middle)** Irradiation of the solution with UVA light (75 s in a photoreactor) generates two new eluting species ( $m/z = 163$  at 8.3 min and  $m/z = 256$  at 11.7 min). **(bottom)** Authentic samples of umbelliferone ( $m/z = 163$  for  $[M+H]^+$ ) and HAPI ( $m/z = 256$  for  $[M+H]^+$ ) elute at identical times as the products formed from irradiation of PC-HAPI. All solutions were prepared at 50  $\mu\text{M}$  in PBS (0.5% DMSO).

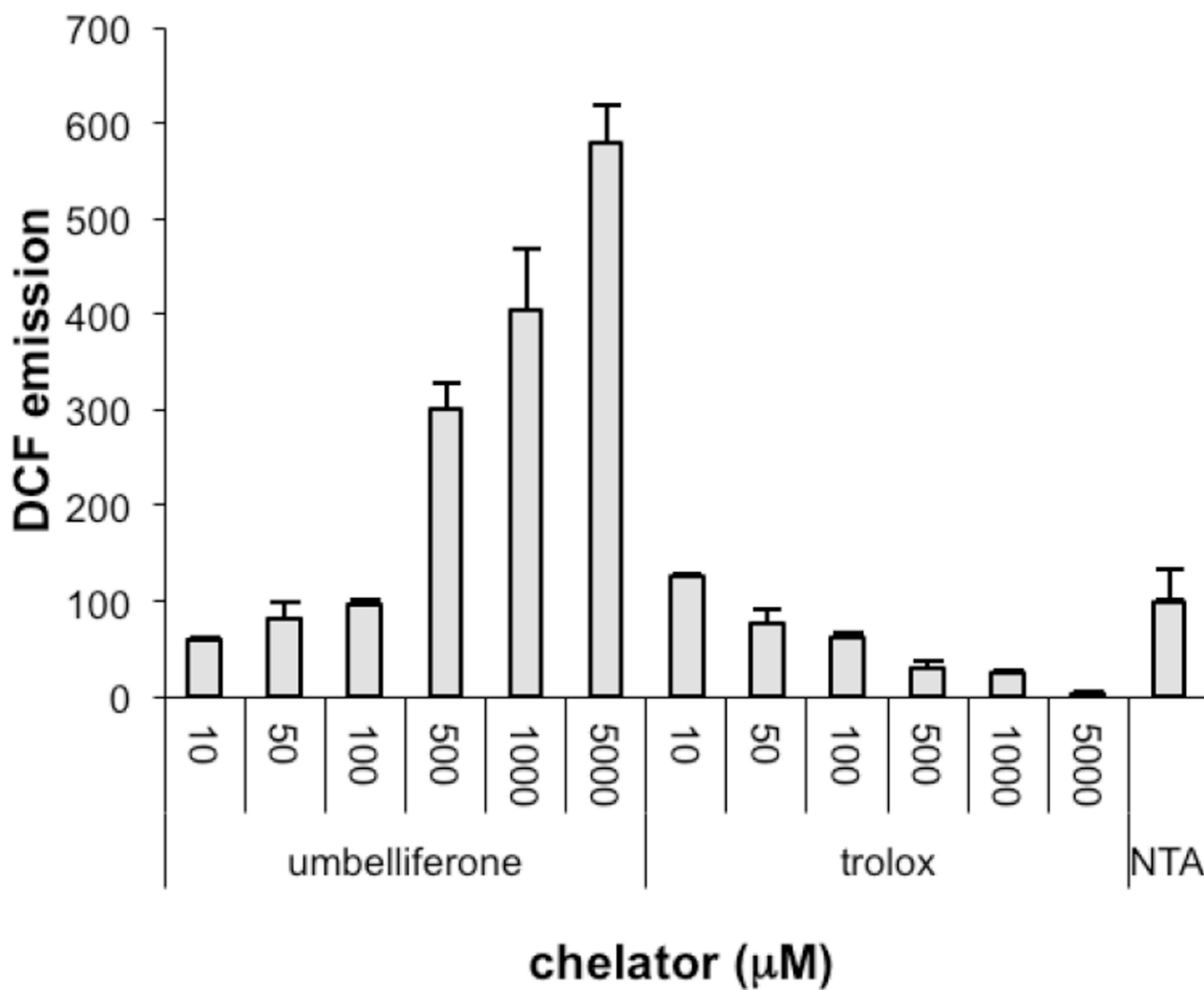


**Figure 4.**

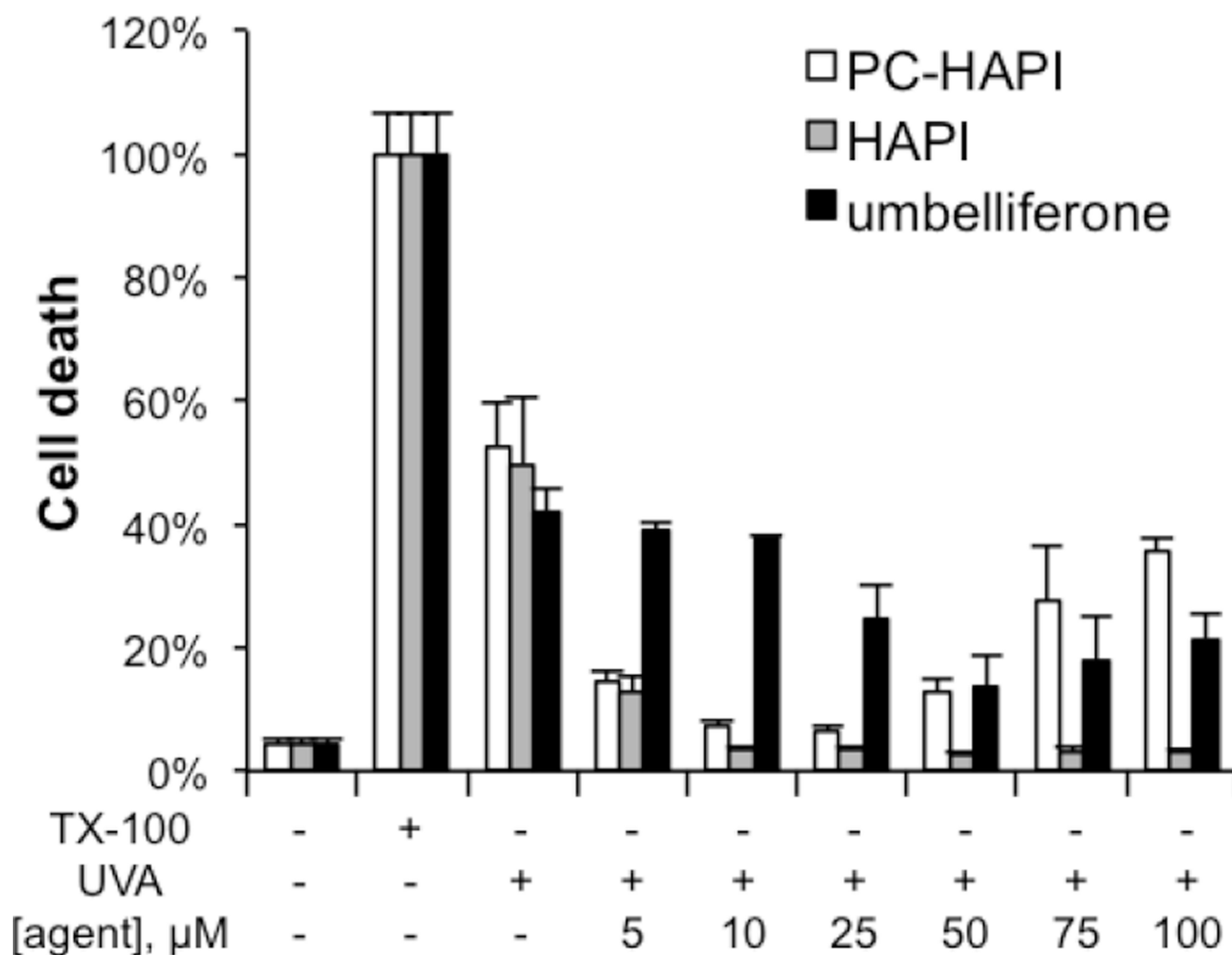
A comparison of calcein fluorescence emission intensity shows that the  $\text{Fe}^{3+}$  affinity of PC-HAPI (PC) is controlled by light. [Calcein] = [Fe] = 2  $\mu\text{M}$ , where Fe =  $[(\text{NH}_4)_2\text{Fe}(\text{SO}_4)_2]$ , which forms  $\text{Fe}^{3+}$ (calcein) complex in situ; [HAPI] = [PC-HAPI] = 10  $\mu\text{M}$  in PBS. Emission recorded 1 h after photolysis (+) for 15 s in a photoreactor ( $\lambda_{\text{max}} = 350 \text{ nm}$ ). Error bars represent standard deviation for conditions run in triplicate.



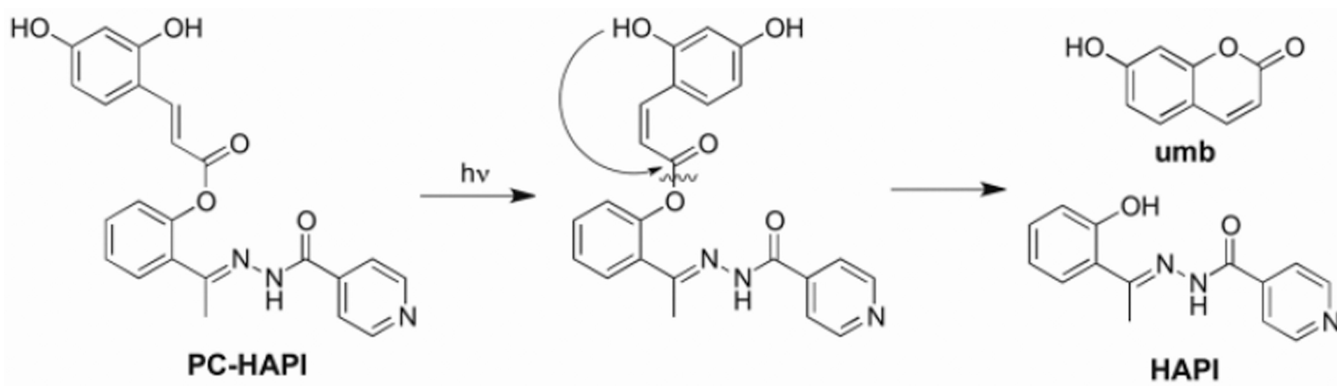
**Figure 5.** Fluorescence assay for Fe-mediated ROS production. HAPI, PC-HAPI, and photolyzed PC-HAPI were tested for their ability to prevent oxidation of H<sub>2</sub>DCF (20 μM) to fluorescent DCF by a cocktail of 10 μM FeCl<sub>3</sub>, 10 μM NTA, 1 mM ascorbic acid, and 1 mM H<sub>2</sub>O<sub>2</sub> in pH 7.4 PBS buffer. All solutions contained 10 μM NTA as a solubilizing Fe<sup>3+</sup> ligand. (“NTA” condition contains NTA with no additional chelators).  $\lambda_{\text{ex}} = 485 \text{ nm}$ ,  $\lambda_{\text{em}} = 535 \text{ nm}$



**Figure 6.** Fluorescence assay of the effect of umbelliferone and trolox on Fe-mediated ROS production monitored by DCF emission. All solutions were prepared in PBS (pH 7.4) with 10 μM FeCl<sub>3</sub>, 10 μM NTA, 1 mM H<sub>2</sub>O<sub>2</sub> and 1 mM ascorbate. Condition labeled “NTA” contains only Fe, NTA, H<sub>2</sub>O<sub>2</sub>, and ascorbate.



**Figure 7.** Cytoprotective effects of PC-HAPI, HAPI and umbelliferone from UVA damage. ARPE-19 cells were pre-treated with various concentrations of HAPI, umbelliferone and PC-HAPI for 2 h, prior to a 40-min UVA exposure with irradiation energy of  $600 \text{ kJ/m}^2$ . Cell death was measured 5 h after UVA irradiation. Triplicates of each treatment group were normalized to the 2% Triton X-100 (TX-100) treated cells.



**Scheme 1.**  
Proposed deprotection mechanism for PC-HAPI